Green biorefinery of Laminaria hyperborea industrial side-streams: Subcritical water extraction optimization via response surface methodology

Downloaded from: https://research.chalmers.se, 2026-08-03 11:22 UTC

Citation for the original published paper (version of record):
Oliver Simancas, R., Leyva-Jiménez, F., Hansen, M. et al (2026). Green biorefinery of Laminaria hyperborea industrial side-streams: Subcritical water extraction optimization via response surface methodology. Bioresource Technology Reports, 35. http://dx.doi.org/10.1016/j.biteb.2026.102928

N.B. When citing this work, cite the original published paper.

research.chalmers.se offers the possibility of retrieving research publications produced at Chalmers University of Technology. It covers all kind of research output: articles, dissertations, conference papers, reports etc. since 2004. research.chalmers.se is administrated and maintained by Chalmers Library

(article starts on next page)

Bioresource Technology Reports 35 (2026) 102928

Contents lists available at ScienceDirect

Bioresource Technology Reports

journal homepage: www.sciencedirect.com/journal/bioresource-technology-reports

Green biorefinery of *Laminaria hyperborea* industrial side-streams: Subcritical water extraction optimization via response surface methodology

R. Oliver-Simancas [a], F.J. Leyva-Jiménez [b], M.D. Hansen [c], I. Bye [c], G. Tizzanini [d], A. Ström [d], A. Jiménez-Quero [a,*]

[a] Division of Industrial Biotechnology, Department of Life Sciences, Chalmers University of Technology, Gothenburg, 41296, Sweden
[b] REQUIMTE/LAQV, Polytechnic of Porto, School of Engineering, Rua Dr. António Bernardino de Almeida, 4249-015, Porto, Portugal
[c] Møreforsking AS, Borgundvegen 340, 6009, Ålesund, Norway
[d] Applied Chemistry, Department of Chemistry and Chemical Engineering, Chalmers University of Technology, Gothenburg, 41296, Sweden

ARTICLE INFO

Keywords:
Brown algae
Industrial sidestreams
Subcritical water extraction
Algal biorefinery
Bioactive compound

ABSTRACT

An integrated response surface methodology (RSM) approach for optimizing subcritical water extraction (SWE) of biopolymers and bioactive compounds from *Laminaria hyperborea* side-streams has been comprehensively developed. Temperature (110–140 °C), solid-to-liquid ratio (1:20–1:35 g:mL), and time (10–20 min) were evaluated on four key responses: yield, soluble protein, phenolic content, and molar mass. Temperature emerged as the most influential factor followed by extraction time and quadratic temperature effects. Building upon these findings, a multi-response optimization identified the targeted optimal conditions, achieving a desirability score of 0.802 under 130.2 °C, 1:28.5 g:ml, and 15.9 min. These conditions recovered up to 22% of the original biomass as an extract rich in fucose and uronic acids, indicative of fucoidan and alginate enrichment. Complementary downstream strategies demonstrated non-cytotoxicity, antioxidant and anti-inflammatory capacities in HaCaT keratinocytes. Findings encourage SWE adoption as a green technology in sustainable algal biorefinery and circular bioeconomy implementation.

1. Introduction

Constant and growing exploitation of natural resources on our planet leads to the imperative need to make all possible efforts in the transition towards circular bioeconomy systems (Gottinger et al., 2020; Schipfer et al., 2024). In this way, society must seek greener alternatives, aiming to provide solutions by efficiently upcycling biomass and side-streams into valuable products, ranging from biofuels, materials, and even bioactive compounds. These approaches reduce reliance on fossil-based resources, while minimizing undervalorized side-stream generation, all supporting sustainable development (Aït-Kaddour et al., 2024; Espro et al., 2021; Liu et al., 2023).

Brown algae (Phaeophyceae) are widely available marine biomasses that have acquired significant attention due to their rich composition of structural polysaccharides as well as bioactive compounds to be used as functional and bioactive constituents in the food, pharmaceutical, and cosmetic sectors (Blunden, 1993; Li et al., 2021; Remya et al., 2022). The relatively low economic resources and human efforts regarding the cultivation of some of these biomasses present significant appeal as sustainable feedstocks (Eger et al., 2023; Smale et al., 2020; Stacey et al., 2021).

Laminaria hyperborea is one of the main brown seaweeds exploited in Europe for alginate extraction, with estimations of around 200.000 tons per year, yielding approximately up to 6000 tons of alginates (Greenhill et al., 2021; Harmsen, 2014). The side-streams generated during the industrial processing activities of brown algae can entail from 25 to 80% of the original biomass, depending on extraction yield and process efficiency (Cebrián-Lloret et al., 2022; Savić Gajić et al., 2024; Wekre et al., 2023).

In the case of *L. hyperborea*, the residual fractions derived from alginate extractions are rich in structural polysaccharides and other valuable metabolites such as mannitol, laminarin and fucoidans (Bojorges et al., 2022; Carvalho et al., 2023). Currently, this fraction remains largely undervalued despite being rich in valuable compounds which represents both an environmental burden but also a lost opportunity for circular-based and high-value valorization applications.

Although traditional extraction methods (e.g., acid, alkaline, or enzymatic treatments) have been applied to algae residues, they often

* Corresponding author.
E-mail address: amparo@chalmers.se (A. Jiménez-Quero).

https://doi.org/10.1016/j.biteb.2026.102928
Received 18 April 2026; Received in revised form 7 June 2026; Accepted 10 July 2026
Available online 17 July 2026
2589-014X/© 2026 The Authors. Published by Elsevier Ltd. This is an open access article under the CC BY license (http://creativecommons.org/licenses/by/4.0/).

involve high chemical usage, limited selectivity and the potential loss of original structure and function of the targeted compounds (Bojorges et al., 2022; Cebrián-Lloret et al., 2022; Moloeznik Paniagua et al., 2024). Due to the intrinsic recalcitrant characteristics of these side-streams, improved extraction techniques need to be explored. In this sense, subcritical water extraction (SWE) is a promising technology to address this issue. This technique uses water in liquid state as a solvent at above 100 °C to solubilize valuable compounds, reducing the need for traditional solvents, ensuring easier downstream processes for the development of the targeted products. The unique properties of water in this subcritical state, including its lower polarity while enhanced diffusion coefficient, may selectively extract bioactive components from agrifood products like polysaccharides, proteins or other functional compounds (Ali et al., 2025; Cheng et al., 2021a; Costa et al., 2023; Majeed et al., 2024; Mohd Thani et al., 2020; Zhu et al., 2011). In addition, and narrowing to the algae side-stream topic, this technique has shown recent promising results on red algae side-streams (Trigueros et al., 2024, 2023), yet, the application of SWE to brown algae side-streams remains largely unexplored.

As a result of this under exploitation, systematic optimization of SWE conditions for these underutilized biomasses is scarce, and the available literature lacks integrated experimental designs to understand the behavior of these technique characteristics regarding compounds recovery and integrity. As such, there is a clear knowledge gap in how to effectively tailor SWE processes for algae side-stream valorization. Addressing this requires exploratory but methodically robust approaches that pave the way for future research and scale-up efforts.

In this context, the present study applies RSM as an optimization and modeling tool to refine SWE conditions for brown algae side-streams. By systematically evaluating the interactions between multiple variables and subsequently fine-tuning the process parameters, the identification of optimal conditions that enhance yield and purity of the targeted compounds are uncovered (Leyva-Jiménez et al., 2022; Myers et al., 2016b; Weremfo et al., 2023). To our knowledge, this is the first study integrating RSM to optimize SWE for brown algal industrial residues, aiming to provide quantitative insight into the behavior of this green technology. The optimized and downstream-processed extracts further revealed notable antioxidant, biocompatible and anti-inflammatory properties, underscoring their potential for value-added applications. This approach supports the circular bioeconomy by promoting waste minimization and the generation of diversified bio-based materials with potential applications in food, pharmaceutical, and cosmetic sectors.

2. Material and methods

2.1. Sample material and treatment

Laminaria hyperborea side-streams were kindly provided by Alginor ASA (Hagaesund, Norway), which were derived from the industrial extraction of fucoidan and alginate. The original algae material was harvested in Haugesund, Norway. The side-stream produced were kept under refrigeration (88.4 ± 1.2% of water content) and then freeze-dried for 72 h in a Labonco Freezone 6 (Labonco Corporation, Missouri, USA) at −48 °C condenser temperature until this water content was reduced to 8.6 ± 0.5%. The sample was milled using an IKA Multidrive (IKA-Werke GmbH & Co. KG, Satufen, Germany) and sieved trough a 2 mm mesh obtaining a homogeneous powder that was stored in a hermetically sealed at room temperature until extraction and analysis.

2.2. RSM-based optimization of SWE

The subcritical extractions from *L. hyperborea* side streams were performed in an Accelerated Solvent Extractor (Thermo Scientific™ EXTREVA™ ASE™, Thermo Fisher Scientific, Sunnyvale, CA, USA). The freeze-dried algal side stream material (0.5 g) was introduced into a stainless-steel cell (10 mL) with both top and bottom cellulose filters and submitted to the extraction process. The physicochemical conditions of the extractions were described in the following paragraphs: a two-step optimization approach was considered as follows: a first stage to determine the temperature working range based on the estimation of the polymerization degree. The second step was performed by RSM to estimate the best combination of temperature, solvent ratio, and extraction time for the responses considered.

2.2.1. Temperature working range

In this case, 13 extracts coming from extraction temperatures ranging from 80° to 200 °C with ten degrees of difference between the extractions were obtained. MilliQ H_2O was used as solvent, and N_2 as pressurizer gas. Solid-to-Liquid ratio (SLR; dry matter biomass grams to solvent milliliters), extraction time (time) and pressure (P) remained static for all the extractions, being SLR = 1:28, $t = 15$ min and $P = 2000$ psi. The extractions were performed in duplicate and the extracts were freeze-dried and stored in refrigeration conditions, hermetically sealed and protected from light until characterization.

2.2.2. Extraction optimization by a RSM approach

The extraction conditions were determined by means of an RSM based on a Central Composite Design 2^3 model with a star and four central points (Table 1). The set ranges for the operational variables were selected based on literature, previous experiences of similar extraction procedures, preliminary screening tests, and operational limitations of the equipment (Alboofetileh et al., 2019; Cheng et al., 2021; Costa et al., 2023; Saravana et al., 2018; Trigueros et al., 2024). In this sense, the selected conditions for the response surface methodology were the following: temperature, 110 to 140 °C; SLR, 1:20–1:35 (g:ml) and time, 10–20 min. The response variables studied were total yield, expressed as percentage of recovered freeze-dried extract relative to the dry weight of the original algal side-stream material (*w*/w %), soluble protein expressed as milligrams of protein per gram of dry extract on a dry matter basis (mg/g_{DM}), Total phenolic content expressed as milligrams of gallic acid equivalents per gram of dry extract on a dry matter basis (mg GAE/g_{DM}), and molar mass reported as weight-average molar mass (Mw) in kilodaltons (kDa). The rest of the operational parameters, such as the number of static extraction cycles: 1; pressure: 2000 psi; pressurizer gas: nitrogen and purging time: 90 s; remained constant for all the extractions. A total of 18 runs including 4 center and star points were proposed to evaluate the effects of the three aforementioned factors (independent variables). The order of the experiments has been fully randomized, sheltering versus the impact of potential lurking variables. Statgraphics centurion version 19 (Statpoint Technologies, Warrenton, VA, USA) was used to create and analyze the model proposed. The α values were determined according to the four center points of the design. A quadratic polynomial model used in the response surface analysis was fitted for each response using Eq. (1):

$$Y = \alpha_0 + \sum_{i=1}^{k} \alpha_i X_i + \sum_{i=1}^{k} \alpha_{ii} X_i^2 + \sum_{i=1}^{k} \sum_{j=i+1}^{k} \alpha_{ij} X_i X_j \quad (1)$$

where Y represents the predicted response; α_0 is the constant coefficient fixing the response at the central point of the experiments (intercept); α_i, α_{ii} and α_{ij} are the regression coefficients of the model representing linear, quadratic, and interaction terms, respectively; X_i and X_j represent the independent variable functions, and k corresponds to the number of variables (k = 3). The statistical parameters used to evaluate the adequacy of the model, and the adjustment of data collected, were the coefficient of determination (R^2), lack-of-fit test, and coefficient of variation (CV).

Table 1
Independent factors defining the experimental conditions of the Central Composite Design 2^3 and their corresponding response values.

Experimental run	Temperature (°C)	SLR (g: ml)	Time (min)	Total yield (w/w %)	Soluble protein material (mg/g_{DM})	Total phenolic content (mg_{GAE}/g_{DM})	Molar mass (kDa)
1	103	27.5	15	18.52	1.07	1.38	130.10
2	110	35	20	19.26	2.18	1.39	97.50
3	110	20	20	18.16	2.25	1.52	74.10
4	110	20	10	16.14	1.08	1.29	79.10
5	110	35	10	17.9	2.30	1.20	103.70
6	125	17	15	19.4	2.49	1.92	78.90
7	125	27.5	8	18.24	1.44	1.47	113.50
8	125	27.5	15	20.14	2.50	2.06	131.20
9	125	27.5	15	19.66	2.60	1.77	134.00
10	125	27.5	15	20.54	2.42	1.89	147.00
11	125	27.5	15	20.08	1.24	1.91	134.00
12	125	27.5	22	21.46	3.62	2.25	87.10
13	125	38.5	15	20.66	1.56	1.75	98.70
14	140	35	10	23.2	3.91	2.22	71.40
15	140	35	20	26.46	3.23	2.70	70.40
16	140	20	10	19.6	3.22	2.11	72.20
17	140	20	20	26.84	2.95	2.81	70.50
18	146	27.5	15	28.72	4.20	2.86	67.00

Experimental runs were originally performed in randomized order to minimize bias, as required by Response Surface Methodology. However, they are presented sorted by ascending temperature for clarity of interpretation.
Molar mass expressed as weight-average molar mass (mw) in kilodaltons (kDa).

2.3. Compositional and structural characterization

2.3.1. Depolymerization estimation by dinitrosalicylic acid assay

The dinitrosalicylic acid (DNS) assay, based on Wood et al. (2012) was used to estimate the concentration of reducing sugars in the extracted material. In a 96 well-plate, 10 µl of sample or standard was mixed with 190 DNS µl reagent in each well. The plate was sealed with adhesive tape and heated in a Bio-Rad T100™ Thermal Cycle (Bio-Rad, Segrate, Italy) thermocycler (ensuring 100 °C for 1 min and 25 °C for 30 s). Reading was performed in a microplate reader at 540 nm after 20s of 1000 rpm stirring. The results were obtained by interpolating the absorbances of the samples with the fucose calibration curve and were expressed as g/L of fucose equivalents.

2.3.2. Extraction yield

The original side-stream sample and the derived aqueous extracts were freeze-dried. The samples were first frozen at −80 °C and then introduced into the freeze-dryer vacuum chamber until the pressure reached stable values around 40×10^{-3} mbar. The room temperature and condenser temperature were 25 °C and −48 °C, respectively. The process was considered finished when the weight of the samples showed less than 0.001 g of difference with respect to the previous measure. Extraction yield was calculated as the ratio between the mass of the recovered freeze-dried extract and the mass of the original dry algal side-stream material.

2.3.3. Soluble protein material

Quantification of soluble proteins was performed using and adapted version of the well-documented Bradford assay (Bradford, 1976). Bovine serum albumin (BSA, fraction V, Sigma-Aldrich, SE) was used as standard to prepare a calibration curve (50–250 µg/mL). Extracts were dispersed with Milli-Q water, followed by continuous rotary mixing at 30 °C, 800 rpm, for 30 min, to ensure adequate dispersion of the soluble protein. Once added Bradford reagent, absorbance was measured at 595 nm using a FLUOstar Omega microplate reader (BMG Labtech, Ortenberg, Germany). Protein content was calculated by interpolation on the BSA curve and expressed as mg/g_{DM} extract.

2.3.4. Total phenolic content

The total phenolic content was estimated by the Folin–Ciocalteu method (Johnson et al., 2022; Singleton et al., 1999). Gallic acid (GA; Sigma-Aldrich, SE) was used as the standard for the preparation of the calibration curve (0.5–200 µg/mL). Once completed the reagents addition step, absorbance was measured at 750 nm using FLUOstar Omega microplate reader, and the total phenolic concentration was determined by interpolation on the GA calibration curve, expressing the result as mgGAE/g_{DM} extract.

2.3.5. Molar mass determination

Size exclusion chromatography combined with multi-angle light scattering (SEC-MALS) was employed to determine the molar mass (Mn and Mw) and dispersity (Đ M) of the samples. An aqueous solvent with 20 mM of $NaNO_3$ and 0.002% *w*/w NaN_3 was used as a mobile phase. The eluent was filtered (0.22 µm MCE membrane filters, MF-Millipore™, Merk) and degassed through sonication prior use. The freeze-dried samples were dispersed in the eluent at a concentration of 1 mg/ml and left stirring overnight. The samples were filtered through a syringe filter (Acrodisc 13 mm minispike with 0.45 µm water-wettable PTFE) and injected in a TSKgel GMPWXL 7.8 × 300 mm column with a particle size of 13 µm. The flow rate used was 0.5 mL/min and the total injection volume was 100 µL.

The HPLC system consists of a degasser (1260 Infinity II Degasser, Agilent), a pump system (1260 Infinity II Quaternary Pump, Agilent), and an autoinjector (1260 Infinity II Vialsampler, Agilent,). Inline filter (Millipore VM 0.05 µm filter) and a ITSKgel guard column PWXL 6.0 × 40 mm with a particle size of 12 µm were placed before the column. The detectors used for the analysis were: a DAWN HELEOS-II multiangle laser light scattering detector and an Optilab rEX refractive index detector. The data was analyzed using the ASTRA software (version 7.3.2). Three replicates per sample were run at a temperature of 50 °C. The dn/dc used was 0.1550 for all the samples.

2.3.6. Monosaccharide composition by High-Performance Anion-Exchange Chromatography with Pulsed Amperometric Detection (HPAEC-PAD) analysis

The carbohydrate composition of the samples was determined after acidic methanolysis and sulfuric acid hydrolysis (Martínez-Abad et al., 2020). The monosaccharides resulting from the hydrolysis were analyzed using HPAEC-PAD with an ICS-6000 equipment (Dionex) equipped with a CarboPac™ PA20 Guard (3 × 30 mm) and an Analytical column (3 × 150 mm). The analytical method conditions were adapted from Thermo Fisher Scientific Application Note 1091 by Basumallick and Rohrer. Analytical standards of fucose, rhamnose, galactose, glucose, xylose, mannose, galacturonic acid, and glucuronic acid

(Sigma-Aldrich, SE) were used for detection and calibration curves (Supplementary material). The cellulose content was estimated by subtracting the glucose obtained by methanolysis from the total glucose content arising from sulfuric hydrolysis (Biermann, 1988).

2.4. Downstream processing

For the dialysis-based methods, a 50 kDa cut-off membrane (Spectrum™ Spectra/Por™ 6, purchased from Fisher Scientific) and ethylenediaminetetraacetic acid (EDTA) was added to chelate multivalent cations present in the sample. For the ethanol precipitation process, equal volumes of cold (−18 °C) 90% ethanol were added to the extract, followed by 5 min centrifugation at 8000 rpm at 4 °C. This step was repeated three times to maximize carbohydrate precipitation. All treated samples were freeze-dried and weighed to calculate yields relative to the original extract.

2.5. Bioactive capacities

2.5.1. Antioxidant capacity

2.5.1.1. 2,2-Diphenyl-1-picrylhydrazyl (DPPH) assay. DPPH methodology was adapted from Sandoval-Gallardo et al. (2020) 0.15 mM DPPH solution in methanol and Trolox standards (20–300 μM) were used to generate a calibration curve (Sigma-Aldrich, NO). Extracts were mixed with the DPPH solution at a 1:9 sample-to-reagent ratio and incubated for 30 min in the dark at room temperature. Absorbance was measured at 540 nm using a Synergy HTX S1LFA microplate reader (BioTek Instruments, USA). The radical scavenging activity was expressed as Trolox Equivalents per dry matter content of each sample.

2.5.1.2. 2,2′-Azinobis(3-ethylbenzothiazoline-6-sulfonic acid) (ABTS) assay. The ABTS radical cation decolorization assay was performed following (Re et al., 1999) with minor modifications. The ABTS radical was generated by reacting 7 mM ABTS salt with 2.44 mM potassium persulfate (Sigma-Aldrich, NO) in 0.01 M phosphate-buffered saline (PBS) and kept in the dark for 16–24 h. The radical solution was diluted in PBS to an absorbance of 0.70 ± 0.03 at 734 nm. Trolox (Sigma-Aldrich, NO) standards (20–300 μM) were used for calibration. Extracts were mixed with the ABTS solution at a 1:19 sample-to-reagent ratio and incubated for 30 min in the dark. Absorbance was measured at 734 nm using a Synergy HTX S1LFA microplate reader, and the results were expressed as Trolox Equivalents (TE) per dry matter (DM).

2.5.1.3. Oxygen radical antioxidant capacity (ORAC) assay. ORAC assay was performed following a BioTek Instruments, Inc. Application Note by Brescia (2021). The reaction used Trolox® standards (3.125–50 μM), sodium fluorescein (SoF, 0.04 μM), and 2,2′-azobis(2-amidinopropane) dihydrochloride (AAPH (100 mM) (all Sigma-Aldrich). Samples and standards were mixed with SoF (1:6 ratio), incubated 30 min at 37 °C, and initiated with AAPH. Fluorescence (Ex 485 nm, Em 528 nm) was monitored every minute for 60 min using a Synergy HTX S1LFA reader. Antioxidant activity was expressed as Trolox Equivalents per dry matter from the area under the curve.

2.5.2. Biocompatibility & anti-inflammatory potential

The cell-promoting bioactivity of the extracts was evaluated using HaCaT human keratinocytes, a widely accepted model of the epidermal barrier for studying cytotoxicity and inflammation-related responses in pharmaceutical and cosmetic applications. Cells were cultured in RPMI-1640 medium (Gibco, USA) supplemented with 10% (*v*/v) fetal bovine serum (FBS), 1% (v/v) penicillin–streptomycin, 100 mM sodium pyruvate, L-glutamine, and glucose, and maintained at 37 °C in a humidified incubator with 5% CO_2. For stimulation, 1×10^4 cells/well were seeded in 96-well plates containing 100 μL complete medium. After 24 h, the medium was replaced, and the cells were pre-treated for 24 h with the algal extracts at 800, 400, 200, or 50 ppm, followed by stimulation with TNF-α (10 ng/mL) and IFN-γ (10 ng/mL) (PeproTech EC Ltd., UK) for another 24 h. Supernatants were collected and stored at −20 °C for cytokine analysis. Cell viability was assessed using the PrestoBlue Cell Viability Reagent (Thermo Fisher Scientific, USA) and the results were expressed as a percentage of untreated HaCaT cells. The interleukin-6 (IL-6) concentration in conditioned media was quantified by ELISA kit (Thermo Fisher Scientific, USA). Briefly, plates were coated overnight with capture antibodies, washed with PBS + 0.05% Tween-20, blocked with 1% BSA in PBS, and incubated with standards and samples in duplicate. After sequential addition of streptavidin–HRP, substrate, and 2 N H_2SO_4 stop solution, absorbance was read at 450 nm using a Synergy HTX S1LFA reader (BioTek Instruments, Agilent, USA).

3. Results and discussion

3.1. Temperature selection range

With the objective of extracting the highest quantity of biopolymers as less depolymerized as possible, a preliminary screening was conducted to identify the adequate working temperature range. *L. hyperborea* is well known as a source of fucoidans and alginate, beyond others. However, at atmosphere pressure, temperatures exceeding 120 °C can promote significant hydrolysis, leading to the potential loss of their biological activities (Álvarez-Viñas et al., 2020; Kopplin et al., 2018). The degree of hydrolysis was estimated by quantification of reducing sugars using the DNS assay (expressed as fucose equivalents). Since alginate degradation products are non-reducing and undetectable by this method, SEC-MALS-RI analysis was additionally performed to determine the average molar mass of the biopolymers or the extracts.

The tested extraction temperature range (80–200° C) revealed significant differences in the degree of biopolymer hydrolysis (Fig. 1a). The total extraction yield increased linearly when rising extraction temperature, with the highest extraction yields at 190 °C (supplementary material), following the trends observed in other species of raw brown algae (Getachew et al., 2022). However, the highest temperatures exhibited the highest concentrations (180–200 °C) of reducing sugars equivalents (82.97–95.86 mg/mL), indicating substantial depolymerization of the extracted polysaccharides containing reducing ends. Conversely, temperatures below 140 °C showed lower reducing sugar concentrations (29.37–49.94 mg/mL). Molar mass distribution data (Fig. 1b) support these trends, showing that both number-average (Mn) and weight-average (Mw) molar mass reach their peak values at 130 °C. At lower temperatures (<110 °C), although hydrolysis seems controlled, the molar mass remains moderate (Mn ≈ 70 kDa; Mw ≈ 80 kDa), potentially indicating incomplete solubilization of the polymers from in the biomass. To achieve the goal of maximizing biopolymer recovery while maintaining under control depolymerization events due to thermal hydrolysis, the working temperature range identified as optimal was 110–140 °C. Studies in similar algae material also determined that temperatures around 130 °C are found to be the optimal ones when targeting algae biopolymer extractions (Saravana et al., 2018).

3.2. RSM analysis of SWE extraction conditions

3.2.1. Model fitting

The experimental results from the SWE trials are summarized in Table 1, serving as an overview of how the responses results varied across the tested variables. In addition, Table 2 presents the statistical evaluation of the fitted quadratic models, including the regression coefficients, *p*-values, and ANOVA results for the main effects but also the interactions among the extraction variables. To assess the model's suitability, the R^2 was utilized as the primary indicator. The R^2 measures the model's effectiveness in predicting the behavior of the response variable.

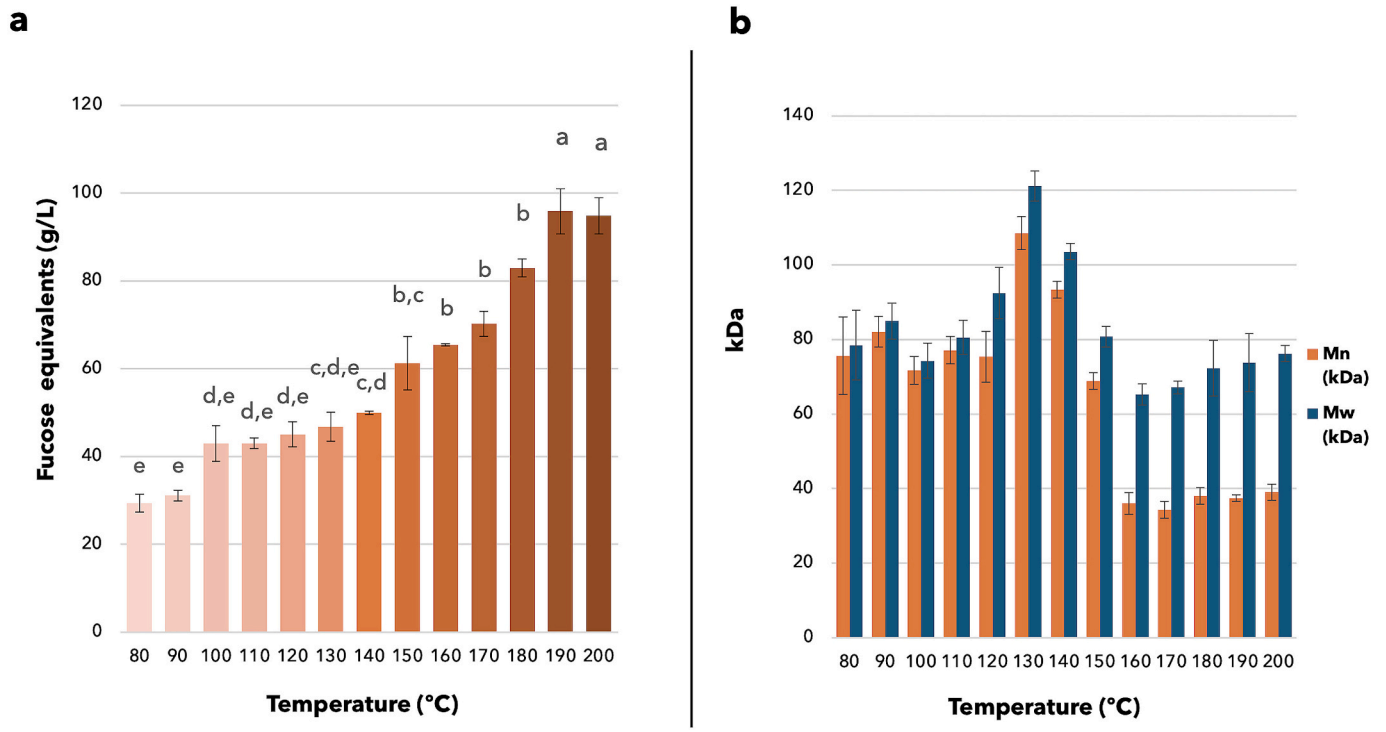

Fig. 1. Effect of extraction temperature on fucose release and molecular weight of the extracts. (a) Reducing sugar content expressed as fucose equivalents (g/L) across a temperature gradient from 80 °C to 200 °C, estimated using the DNS assay. Different letters denote significant differences based on Student–Newman–Keuls post hoc analysis ($p < 0.05$). (b) Number-average (Mn) and weight-average (Mw) molecular weights (kDa) of the extracted polysaccharides, showing a peak at 130 °C before declining due to thermal depolymerization. Data are shown as mean ± SD ($n = 3$).

Table 2
Multiple linear regression and ANOVA results of the parameters and interactions of the analyzed responses, from the SWE of *Laminaria hyperborea* side-stream.

Parameters & interactions	Total yield			Soluble protein material			Total phenolic content			Molar mass		
	Mean square	F-ratio	P-value	Mean square	F-ratio	P-value	Mean square	F-ratio	P-value	Mean square	F-ratio	P-value
Temperature (A)	127.1730	980.51	0.0001[a]	8.2010	20.04	0.0208 [a]	3.5708	264.60	0.0005[a]	2110.3700	41.98	0.0075[a]
SLR (B)	5.1618	39.80	0.0080[a]	0.0569	0.14	0.7340	0.0183	1.36	0.3279	469.6340	9.34	0.0552
Time (C)	28.3170	218.33	0.0007[a]	0.8465	2.07	0.2459	0.6039	44.75	0.0068[a]	218.7510	4.35	0.1283
AA	18.2070	140.38	0.0013[a]	0.5826	1.42	0.3185	0.0668	4.95	0.1125	2425.0500	48.23	0.0061[a]
AB	0.0162	0.12	0.7472	0.0038	0.01	0.9290	0.0070	0.52	0.5232	298.9010	5.95	0.0926
AC	6.3368	48.86	0.0060[a]	0.4955	1.21	0.3515	0.0700	5.19	0.1072	9.0313	0.18	0.7002
BB	0.6808	5.25	0.1059	0.0095	0.02	0.8885	0.0218	1.62	0.2931	4020.1600	79.96	0.0030 [a]
BC	2.6912	20.75	0.0198	0.3608	0.88	0.4170	0.0088	0.65	0.4793	0.0313	0.00	0.9817
CC	1.1332	8.74	0.0597	0.3797	0.93	0.4064	0.0120	0.89	0.4156	2187.4000	43.51	0.0071[a]
	R-squared = 97.5829%			R-squared = 71.766%			R-squared = 98.4421%			R-squared = 93.3629%		
	Standard Error of Est. = 0.3601			Standard Error of Est. = 0.73333			Standard Error of Est. = 0.0931			Standard Error of Est. = 7.0906		
	Mean absolute error = 0.4086			Mean absolute error = 0.4083			Mean absolute error = 0.0454			Mean absolute error = 5.50853		
	Lack of fit = 4.3093 (p-val = 0.0750)			Lack of fit = 3.0744 (p-val = 0.3916)			Lack of fit = 0.0288 (p-val = 0.8099)			Lack of fit = 689.6030 (p-val = 0.2178)		
	Highest CV < 3.69			Highest CV < 38.37			Highest CV < 5.50			Highest CV < 14.15		

Parameters and interactions marked with superscript [a] are statistically significant at the $p < 0.01$ level for Total Yield, Total Phenolic Content and Molar mass and $p < 0.05$ for Soluble Protein Material.
Coefficients of Variation (CV) full dataset can be found in the Supplementary Material.
Molar mass expressed as weight-average molar mass (mw) in kilodaltons (kDa).

A strong correlation was observed for this parameter in the case of the response variables analyzed using the experimental model. Additionally, the CV was considered, where a value below 10% is known to be regarded as an acceptable and reproducible system (Liyanapathirana and Shahidi, 2005). The lack-of-fit metric highlights the alignment between the central composite design (CCD) and the response variables: how well the model fits the experimental data by comparing the variability of the residuals to the pure error from replicated data. In addition, multiple linear regression (MLR) was employed to develop regression equations and generate response surface plots (Fig. 2) which visually illustrate the behavior of the variables on each studied response (Myers et al., 2016a).

3.2.2. *Analysis of the studied model responses*

3.2.2.1. Total yield. The yields obtained ranged from 16.14 to 28.72% and the variable temperature (A) was the factor exhibiting the most significative impact regarding this response, as shown by its high significant p-value ($p < 0.0001$) and large F-ratio (980.51) (Table 2). This means that SWE can recover almost one-third of the original side-stream

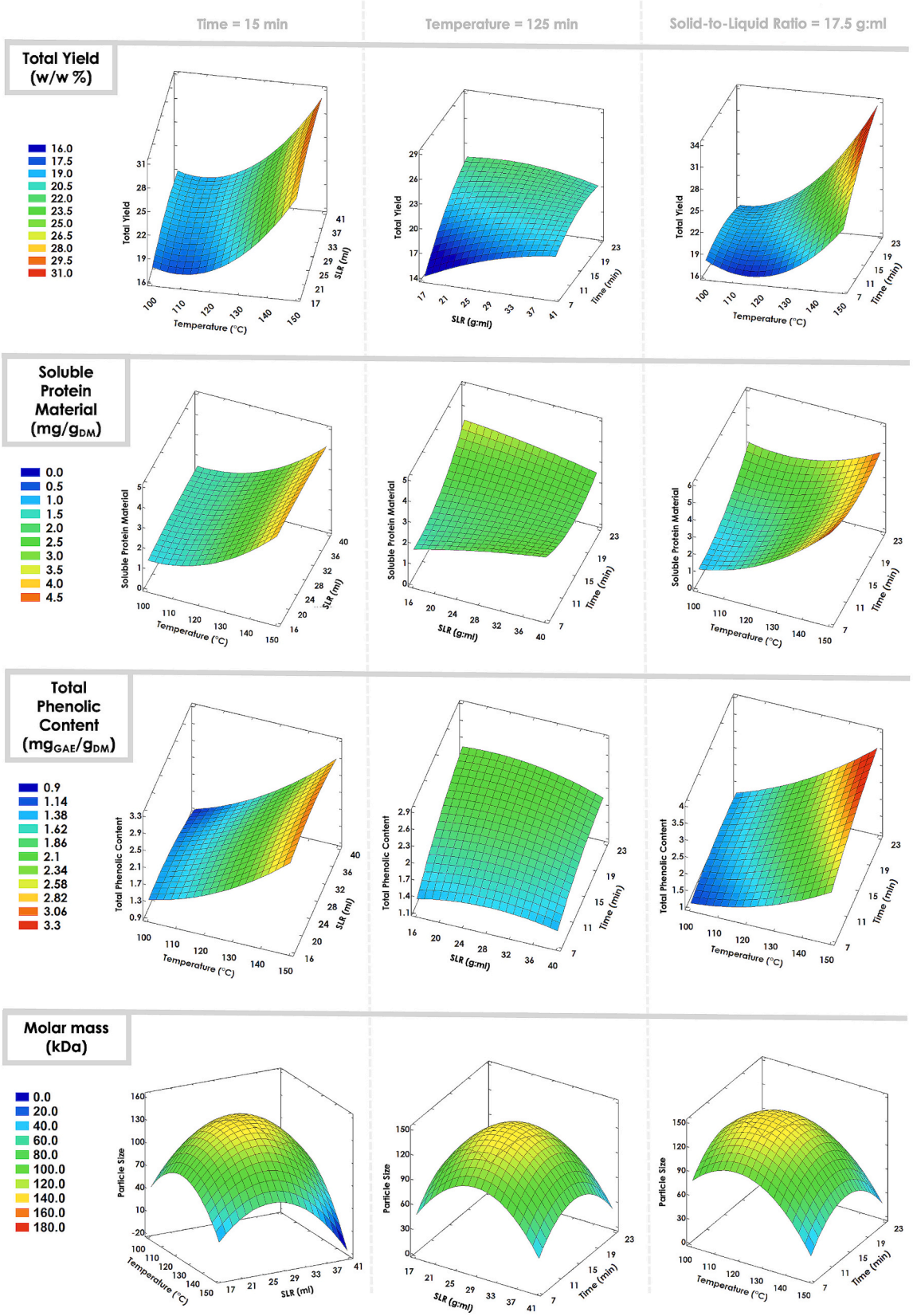

Fig. 2. Response surface plots for individual responses at fixed levels of each variable. Three-dimensional response surface plots showing the effects of temperature, time, and solid-to-liquid ratio (SLR) on: total yield (w/w %), soluble protein material (mg/gDM), total phenolic content (mgGAE/gDM), and particle size (kDa). Each row represents a different response, while columns fix one of the three variables: (left) time = 15 min, (middle) temperature = 125 °C, (right) SLR = 17.5 g:ml. Color gradients indicate predicted values based on RSM models.

material, depending on temperature used for extraction. This response shows the linear role of temperature in enhancing extractability, thus the recovery of algae compounds. These values align with results from other agricultural side-streams (Cheng et al., 2021; Getachew et al., 2022; Yilmaz-Turan et al., 2023). Regarding the model performance and reliability, the statistical analysis results indicate that the studied model can effectively explain the variability of the total yield, as proven by both R^2 and adjusted R^2 values of 97.57% and 94.83%, respectively. It can confirm that for the total yield, this model is robust and accounts for nearly all the observed variation in this response, observing minimal overfitting (as can be seen in the low differences found with the adjusted R^2). Furthermore, the lack-of-fit test was non-significant ($p = 0.075$), the highest CV derived from the predicted and the experimental runs was 3.69%. In addition, the low values displayed by both the mean absolute error (0.4086) and standard error of estimate (0.3601) support the model's overall reliability. The predicted R^2 of 79.42%, though lower, shows that the model maintains a good predictive capability, indicating its utility for practical applications (Myers et al., 2016b). Time (C) was also a significant factor ($p < 0.001$) but SLR (B) though significant, presents a weaker impact on the yield response, potentially due to enhanced diffusion of the targeted compounds at higher SLR. In addition, the quadratic effect of temperature (AA, $p < 0.05$) suggests that the yield response cannot be considered linear as a plateau can be observed at intermediate temperatures. Interactions between the rest of the factors were less impactful in general terms, but the interaction between temperature and time (AC) was significant ($p < 0.05$), indicating a synergistic relationship that should be carefully considered. Fitting experimental data to a reduced model while keeping only the significant factors provided the following model equation (Eq. (2)):

$$Yield = 100.774 - 1.648A + 0.551B - 0.297C + 0.007AA + 0.0119AC \quad (2)$$

3.2.2.2. Soluble protein material. The soluble protein material content among the runs accounted from 1.07 to 4.20 mg/g_{DM} confirming the low protein abundance in the starting material. The model explains a moderate portion of the observed variability, with an R^2 and adjusted R^2 values of 71.77% and 40.0% respectively. In addition, the rest of the statistical parameters indicate moderate predictive reliability and robustness of studied model.

Among the evaluated factors, temperature (A) was the only statistically significant variable ($p = 0.0208$). Overall, soluble protein recovery had low responsiveness to the tested SWE parameters, which may reflect a low initial protein content of the side-stream and the potential influence of factors not captured within the proposed model. Due to this, soluble protein material was not considered a key response variable in subsequent analyses.

3.2.2.3. Total phenolic content (TPC). The total phenolic content obtained from the experimental run varied from 1.68 to 3.19 mg_{GAE}/g_{DM} extract. The statistical analysis for TPC indicates a highly reliable model, as evidenced by the R^2 of 98.44% and an adjusted R^2 of 96.69%. These values demonstrate that the model is highly robust, accounting for nearly all of the observed variation with minimal overfitting. Additionally, the lack-of-fit test was non-significant ($p = 0.8099$), and the CV was low at 5.49%, which further supports the model's consistency. The mean absolute error (0.0454) and standard error of estimate (0.0931) were also low, reinforcing the model's overall reliability.

When analyzing the effect of individual factors, temperature (A) was by far the most influential, as demonstrated by its highly significant *p*-value (0.0005) and time (C) also had a statistically significant impact, though it was less pronounced. For the rest of the studied factors, SLR (B) and all interaction and quadratic terms, those were statistically non-significant. These results support a predominantly linear trend in phenolic content variation (Fig. 2), where increased temperature and prolonged extraction time favor compound release and/or formation (Getachew et al., 2022; Ko et al., 2020; Plaza et al., 2010a, 2010b; Yu et al., 2014). Fitting the experimental data to a reduced model while retaining only the significant variables resulted in the following predictive equation (Eq. (3)):

$$TPC = 5.007 - 0.091A - 0.04C \quad (3)$$

3.2.2.4. Molar mass. The average molar mass distribution ranged from 50 to 90 kDa. Statistical results show that the model can reliably explain the variation in molar mass, as evidenced by a high R^2 of 93.36% and an adjusted R^2 of 85.90%. The lack-of-fit test was non-significant ($p = 0.2178$) and the highest coefficient of variation accounted for an acceptable 14.15% confirming that the model adequately describes the experimental data.

In terms of the effects of individual factors, temperature (A) was again statistically significant ($p = 0.0075$), confirming its leading role in driving molar mass variation. Additionally, the quadratic effects of temperature (AA), SLR (BB) and time (CC) were all significant, suggesting that molar mass does not respond linearly to the variables range, instead, it showcases an optimum region rather than a simple increase or decrease across the tested range. These results reflect the interplay between thermal and mass transfer effects on the extracted particles: intermediate extraction conditions favored the recovery of larger macromolecules (optimal region), whereas conditions at the lower end tended to yield lower molar masses due to incomplete extraction, and conditions at the higher end promoted degradation and consequently reduced molar mass (Shao et al., 2011; Yang et al., 2013) as illustrated in Fig. 2. Therefore, for this response, fitting the experimental data to a reduced model while retaining only the significant terms provided the following equation (Eq. (4)):

$$Molar\ mass = -1588.5 + 19.743A + 0.0774AA - 0.404BB - 0.661CC \quad (4)$$

3.2.3. Multiple response optimization

To identify the optimal SWE conditions that simultaneously balance all target responses, a multiple response optimization was performed using a desirability-based approach based on the process objectives and statistical significance, thanks to the previously analyzed parameters that demonstrated robustness, reliability, and low residual error across the individual models (Myers et al., 2016a). In this sense, the optimization aimed to maximize total yield, total phenolic content, and molar mass (impact value = 3), while minimizing soluble protein material (impact value = 1), in line with the process objectives and the reliability of the individual model responses. Among these, molar mass carried the highest weighting (1.0), followed by yield (0.5), and the remaining responses (0.1 each).

The optimal process conditions were identified as follows: temperature = 130 °C, SLR = 1:28.55 g:ml, and extraction time = 15.88 min, achieving a desirability score of 0.802. This score reflects how the selected conditions satisfy all response goals simultaneously on a scale from 0 (completely undesirable) to 1 (fully desirable) Under these optimal conditions, the predicted values were: Yield = 21.98%, Soluble Protein = 2.52 mg/g, Total Phenolic Content = 2.16 mg GAE/g, and molar mass = 170 kDa (Fig. 3).

To validate the model, an additional extraction was conducted under these optimal conditions in triplicate to assess the coefficients of variation (CV) between predicted and experimental values (Supplementary material). The CV values for the responses after performing the optimal extraction were below 5% (except for soluble protein, confirming the weaker model fit and sensitivity, as previously discussed), supporting the predictive reliability of the proposed conditions and highlighting the effectiveness of the multiple optimization approach.

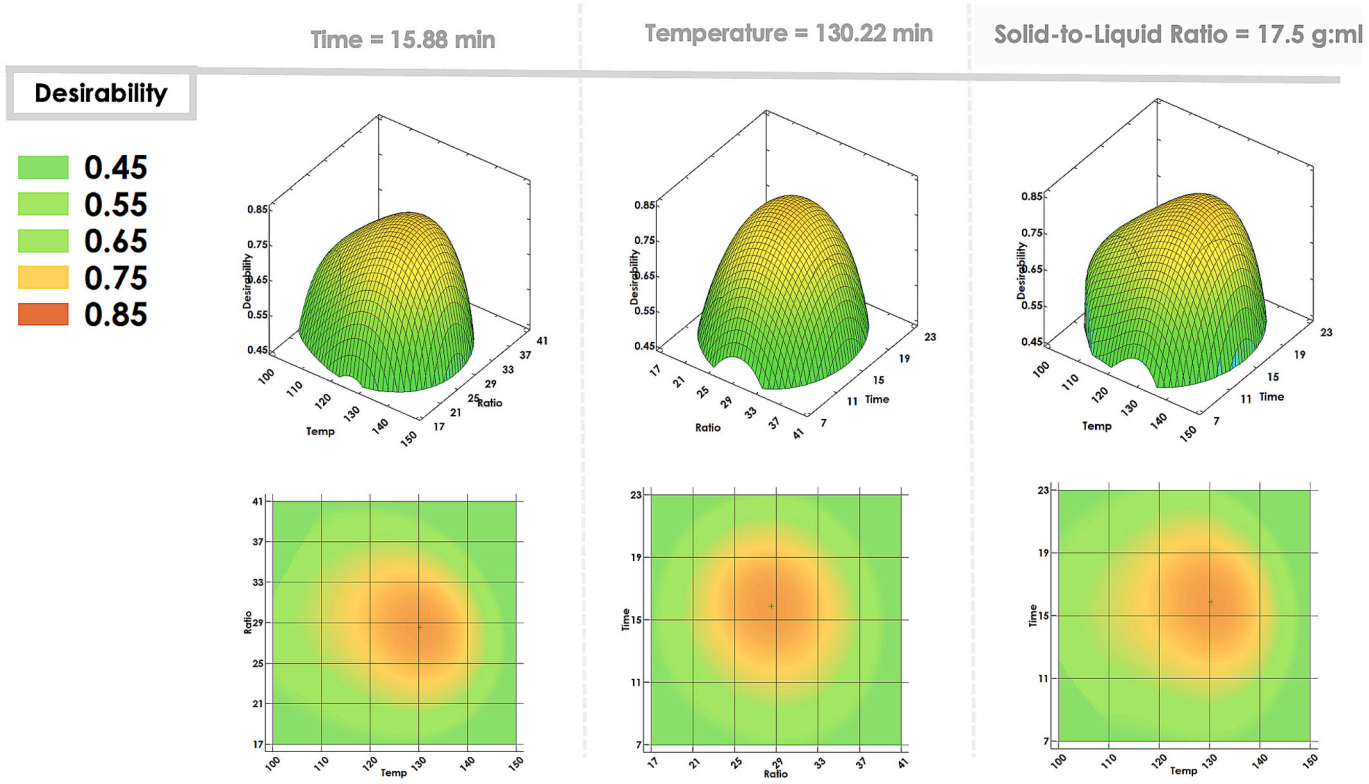

Fig. 3. Desirability plots for multi-response optimization of subcritical water extraction. Three-dimensional (top) and contour (bottom) plots of overall desirability function combining four responses: yield, soluble protein, total phenolic content, and particle size. Each plot shows the effect of two variables while the third is fixed at optimal conditions: (left) time = 15.88 min, (middle) temperature = 130.22 °C, (right) SLR = 28.05 g:ml. Maximum desirability (orange area) is observed around the optimal point.

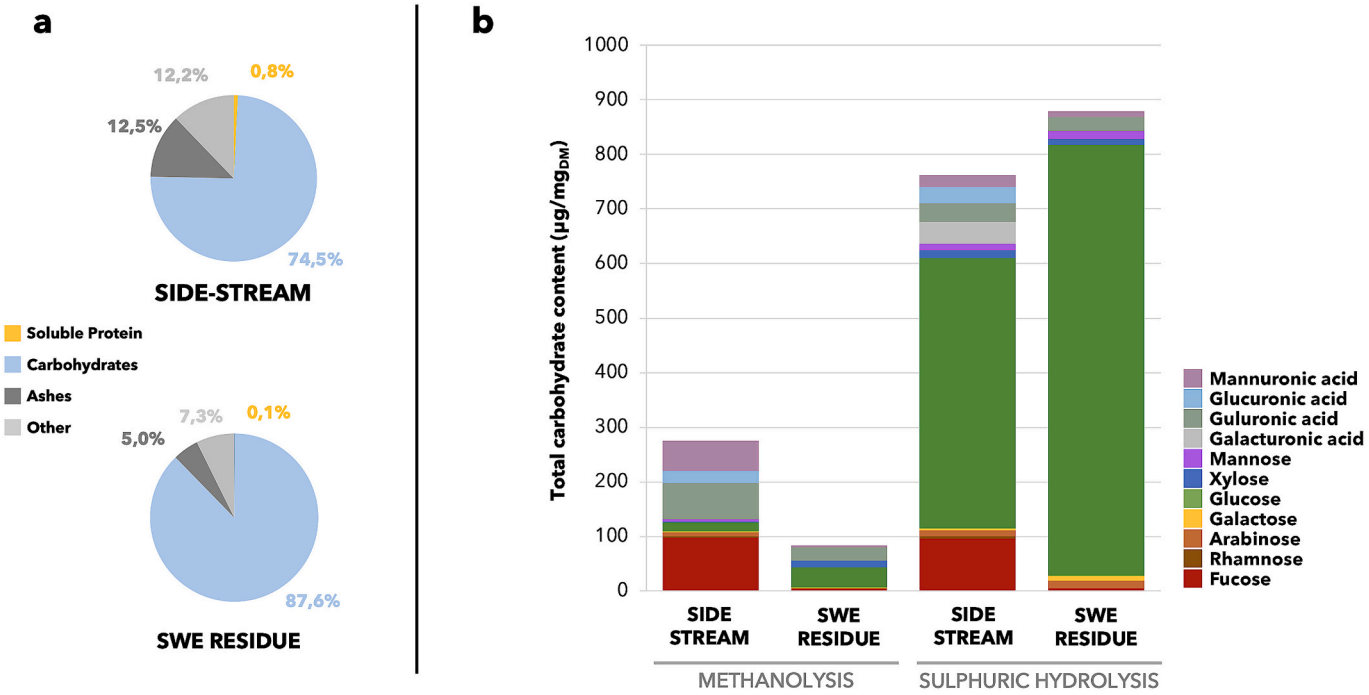

Fig. 4. Compositional analysis of raw and extracted *Laminaria hyperborea* side-stream biomass. (a) Proximate composition (carbohydrates, proteins, ashes, and other components) of the raw side-stream and the residue after SWE, expressed as % of dry matter. (b) Monosaccharide profiles determined by methanolysis and sulfuric acid hydrolysis, showing total and individual sugar content (µg/mgDM) before and after extraction. Data are shown as mean ± SD (n = 2).

3.3. Integrated characterization of the biomass, residue and downstream fractions

This section describes the composition of the starting biomass, the residue remaining after SWE, the optimized extract, and the fractions obtained by the proposed downstream strategies. Together, these results provide an integrated view of how the biomass is distributed across the different biorefinery streams.

3.3.1. Characterization of the original biomass and residue after extraction

Fig. 4a illustrates the proximate composition of the raw L. *hyperborea* side-stream (SIDE-STREAM) and its corresponding residue after the optimal subcritical water extraction (SWE RESIDUE). The original biomass is notably rich in carbohydrates (glucose, fucose and uronic acids), which account for 74.5% of its dry matter, with minor contributions from soluble protein (0.8%), ashes (12.5%), and other components (12.2%). This remaining 12.2% comprises mainly non-protein nitrogen (NPN) since it corresponds to 2.53% nitrogen content determined by elemental microanalysis when 4.75 is used as conversion factor (Angell et al., 2016). Total lipid content was analyzed but the results were shown below detection limits, likely due to their low abundance in the original biomass (Garcia-Vaquero et al., 2021; Schiener et al., 2015) together with its removal during prior industrial processing.

Monosaccharide profiling was performed by acidic methanolysis and sulfuric acid hydrolysis, as shown in Fig. 4b. Methanolysis hydrolyzes only soluble polysaccharides, while sulfuric acid hydrolysis enables the quantification of both soluble and structural carbohydrates. Both methods were analyzed complementarily to obtain a complete view of the carbohydrate composition. In this sense, acidic methanolysis showed fucose (97.4 ± 4.0 $\mu g/mg_{DM}$), guluronic acid (66.6 ± 7.1 $\mu g/mg_{DM}$) and mannuronic acid (55.2 ± 7.7 $\mu g/mg_{DM}$) as the dominant monosaccharides in the composition, exerting a total carbohydrate content of 275.5 $\mu g/mg_{DM}$ (Fig. 4b). These results are in line with those found in the literature in which reports the presence of soluble polysaccharides such as fucoidans and alginate fragments in similar biomasses (Bojorges et al., 2022; Mohd Fauziee et al., 2021). After SWE, these values sharply decreased in the residual fraction, and the total carbohydrate content fell to 83.6 $\mu g/mg_{DM}$, indicating that most of the targeted soluble polysaccharides were effectively depleted during SWE. Sulfuric acid hydrolysis provided further information regarding the monosaccharides derived from the structural carbohydrates. The high glucose content (495.2 ± 5.9 $\mu g/mg_{DM}$) indicated the important presence of cellulose compositing this seaweed cell wall (Onyianta et al., 2020; Schiener et al., 2015). As expected, this value increased after the SWE up to 798.3 ± 6.4 $\mu g/mg_{DM}$ demonstrating that SWE efficiently recovers soluble polysaccharides from the *L hyperborea* side-stream biomass while enriching the residual material in cellulose, which may serve as a purified feedstock for further applications (Baghel et al., 2021).

3.3.2. Characterization of the optimal extract and study of the downstream process

The optimized extract was characterized by Size-Exclusion Chromatography coupled with Multi-Angle Light Scattering and Refractive Index detection (SEC-MALS-RI), revealing three distinct populations: Population 1 (Mn = 273 ± 6 kDa, Mw = 497 ± 26 kDa), respectively; Population 2 (Mn = 122 ± 3 kDa, Mw = 127 ± 6 kDa) and Population 3 (<50 kDa). Population 2 showed the strongest in both the Refractive Index RI and Multi-Angle Light Scattering (MALS) detectors. In contrast, Populations 1 and 3 exhibited almost nonexistent light scattering and reduced RI signals. For the population 1 this can be attributed to the high hydration level of these polymerized molecules, which limits their capacity to scatter light effectively in solution or show any refractive index. Whereas for the population 3, the average-molecular-weight was not big enough to scatter the light, and the reduced refractive index showed the reduced content of the components present in this fraction.

These individual populations were analyzed by acid methanolysis-HPAEC-PAD to screen their monosaccharide composition (Fig. 5a). Fucose, glucuronic, guluronic and mannuronic acid were primarily found in Populations 1 and 2, indicating that the extracted polysaccharides predominantly formed fucoidan and alginate macromolecules of at least ~120 kDa. Population 3 contained only trace levels of these sugars, suggesting the presence of oligosaccharides or degradation products.

To further purify the extract and remove soluble contaminants, two alternative strategies were explored: EDTA-assisted dialysis (50 kDa cut-off) and ethanol precipitation. EDTA chelates multivalent cations that promote alginate crosslinking, avoiding aggregated polymer networks (Draget et al., 1997; Pan et al., 2022; SMIDSROD and SKJAKBRK, 1990). Ethanol precipitation recovers high-molecular-weight polysaccharides, while low-molecular-weight ones and other solubilized components and contaminants may disappear with the supernatant (Hahn et al., 2012).

In this sense, recovery yields were 57.5 ± 1.4% (EDTA-dialyzed) and 75.2 ± 4.5% (ethanol-precipitated). Both explored downstream processes purified the extract by eliminating Population 3 (<50 kDa). The EDTA-dialyzed fraction exhibited the highest Mw for Population 1 (672 ± 18 kDa), suggesting that disrupting ionic associations may favor recovery of larger alginate and/or fucoidan assemblies. In contrast, ethanol-precipitated showed the largest values for Population 2 (Mn = 187 ± 37 kDa; Mw = 196 ± 48 kDa. Total carbohydrates content reached 675 ± 67 $\mu g/mg_{DM}$ (EDTA-dialyzed), and 857 ± 16 $\mu g/mg_{DM}$ (ethanol-precipitated). Fig. 5b shows how EDTA-dialysis enriched the downstreamed extract in fucose and uronic acids while ethanol-precipitation displayed a monosaccharide composition closer to the original SWE extract (control).

In summary, the two alternative routes may serve as downstream processes to purify and maximize the valorization of high-molecular-weight polysaccharides: EDTA-assisted dialysis provides greater selectivity for high-molecular-weight fucoidan/alginate enrichment, whereas ethanol precipitation affords greater mass recovery with a reduced compositional selectivity (Table 3).

4. Bioactivity potential

A wide array of assays measuring in vitro antioxidant potential were performed, including DPPH, ABTS, ORAC as well as an estimation of the Total Polyphenolic Content (TPC) by the Folin-Ciocalteu method. Each method relies on a different mechanism of antioxidant activity (e.g., hydrogen atom transfer, single-electron transfer, radical scavenging) for comprehensive assessment of antioxidant performance on the control extract and the two downstreamed versions. As summarized in Table 4, all samples exhibited measurable antioxidant activity with EDTA-dialyzed sample outperforming in electron-transfer–based assay.

In-vitro cellular assays were conducted to determine whether the downstream strategies could preserve or improve the revalorized extract's potential anti-inflammatory properties. The keratinocyte cell line HaCaT was pretreated with the different samples and exposed inflammatory stimuli. Any of the of the tested samples significantly affected cell viability compared to untreated controls, confirming their non-cytotoxic behavior across the tested concentration range (50–800 ppm) as shown in Fig. 6a. To evaluate the cellular response to inflammation, IL-6 secretion was measured. IL-6 is a proinflammatory cytokine, where prolonged secretion can contribute to chronic inflammation (Hunter and Jones, 2015). As shown in Fig. 6b, the control extract and both downstreamed ones reduced IL-6 secretion in a dose-dependent manner, outstanding ethanol-precipitated extract since this sample exhibited inhibition levels comparable to those of the commercial fucoidan used as the reference. Compositional-bioactivity correlation analysis reveals fucose-rich fractions (SEC-MALS/HPAEC-PAD) as primary drivers of observed activities since fucoidan polysaccharides are well documented for both antioxidant and anti-inflamatory effects in various cellular models (Ahmad et al., 2021; Apostolova et al., 2020).

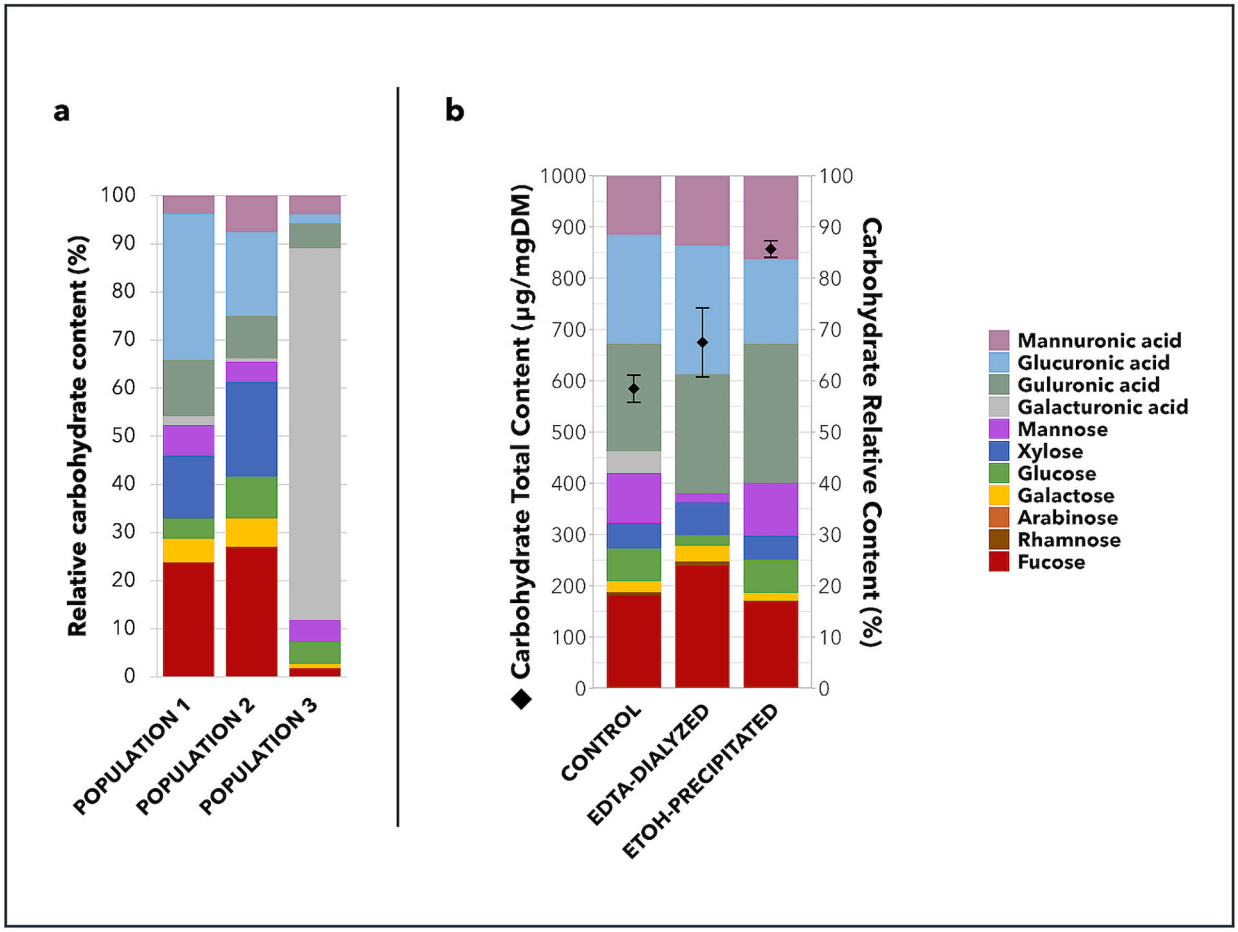

Fig. 5. Monosaccharide profiling of SEC-separated extract fractions and downstream processed samples. (a) Relative carbohydrate composition (%) of three molar mass populations isolated from the optimal SWE extract using SEC-MALS-RI. (b) Total (bars, left axis) and relative (lines, right axis) carbohydrate content in the crude extract (control) and downstream samples: EDTA-dialyzed and ethanol-precipitated. Data are shown as mean ± SD (n = 3).

Table 3
Average molar mass distributions (Mn;Mw) and dispersity (ĐM) of the populations found in the control and the proposed downstream processes determined by SEC-MALS-RI.

	Population 1			Population 2		
	Mn	Mw	ĐM	Mn	Mw	ĐM
CONTROL	273 ± 6 b	497 ± 26 b	2 ± 0	122 ± 3 c	127 ± 6 b	1 ± 0
EDTA-DYALIZED	323 ± 8 a	672 ± 18 a	2 ± 0	130 ± 2 b	137 ± 3 b	1 ± 0
ETOH-PRECIPITATED	127 ± 2 c	256 ± 1 c	2.0 ± 0.0	187 ± 37 a	196 ± 48 a	1 ± 0

Different letters indicate statistically significant differences between the downstream processes as determined by the Student-Newmals-Keuls (SNK) post hoc test ($p < 0.05$).

Table 4
Radical scavenging (DPPH, ABTS, ORAC) and total phenolic content (TPC) of control and the proposed downstream processes.

	DPPH (µmol TE/g)	ABTS (µmol TE/g)	ORAC (µmol TE/g)	TPC (mg GAE/g)
CONTROL	181.44 ± 19.51 b	1055.25 ± 79.98 a	1369.30 ± 19.60 a	48.61 ± 1.24 b
EDTA-DYALIZED	292.31 ± 12.85 a	1210.34 ± 86.23 a	795.80 ± 50.70 b	79.96 ± 1.65 a
ETOH-PRECIPITATED	100.39 ± 4.09 c	578.98 ± 2.15 b	479.00 ± 47.10 c	34.41 ± 1.00 c

Different letters indicate statistically significant differences between the downstream processes as determined by the Student-Newmals-Keuls (SNK) post hoc test ($p < 0.05$).

Overall, these findings validate SWE-RSM as a feasible strategy for *L. hyperborea* side-stream valorization, with EDTA-dialysis and ethanol precipitation emerging as complementary downstream routes yielding efficient and non-cytotoxic fractions suitable for bioactive-oriented application developments.

5. Conclusions

Subcritical water extraction (SWE) proved to be an effective green strategy for the valorization of *L. hyperborea* side-streams, enabling recovery of nearly ¼ of the original biomass maximizing the extracted polymers molar mass. Temperature was identified as the most influential parameter, and the proposed models successfully predicted all responses except protein extraction. Optimal conditions (130.2 °C, 1:28.5 g:mL, 15.9 min) yielded ~22% extract rich in polysaccharides selectively solubilizing fucoidan- and alginate-rich fractions. SEC-MALS-RI revealed three molecular-weight populations, with dominant fucoidan/alginate macromolecules above ~120 kDa. EDTA-assisted dialysis and ethanol precipitation efficiently removed low-molecular-weight fractions, offering complementary downstream routes with distinct selectivity and recovery. Both non-cytotoxic purified extracts showed in vitro antioxidant and anti-inflammatory activities, revealing that bioactivity is mainly driven by the revalorized polysaccharides. This

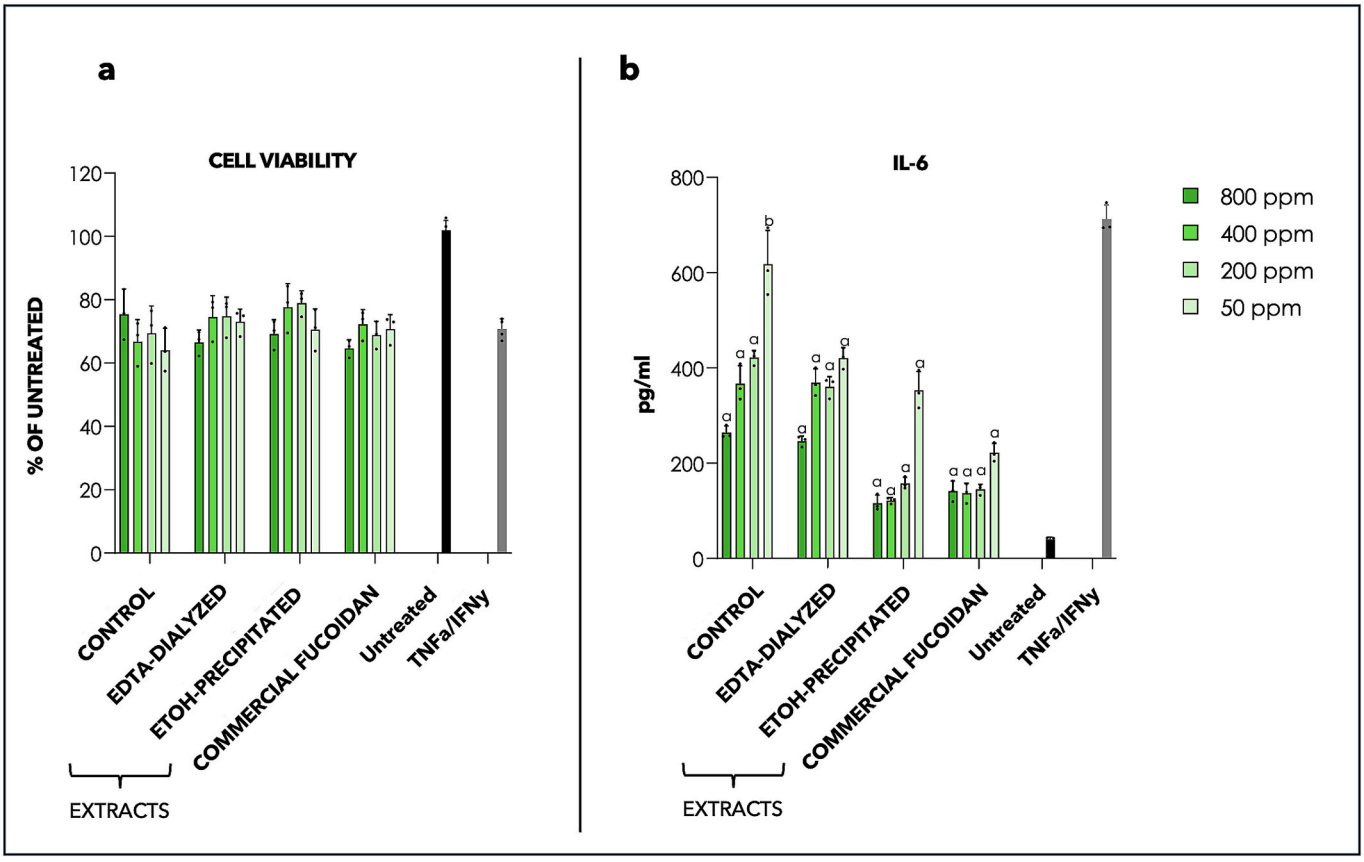

Fig. 6. Effects of downstreamed extracts on keratinocyte viability and IL-6. (a) Cell Viability (% of untreated). (b) IL-6 (pg/mL) after TNFα/IFNγ. Treatments: crude extract (control) EDTA-dialyzed, ethanol-precipitated, and commercial fucoidan at 50–800 ppm; "Untreated" and "TNFα/IFNγ" tested as references. Bars indicate mean ± SD ($n = 3$). Different letters denote significant differences based on Student–Newman–Keuls post hoc analysis ($p < 0.05$).

exploratory study lays a solid foundation for integrating SWE into sustainable algal biorefinery schemes. These insights motivate further structural/functional characterization of the revalorized material alongside the techno-economic scale-up towards commercial implementation.

CRediT authorship contribution statement

R. Oliver-Simancas: Writing – review & editing, Writing – original draft, Visualization, Validation, Methodology, Investigation, Formal analysis, Data curation, Conceptualization. **F.J. Leyva-Jiménez:** Writing – original draft, Methodology, Formal analysis. **M.D. Hansen:** Methodology, Formal analysis, Data curation. **I. Bye:** Methodology, Formal analysis, Data curation. **G. Tizzanini:** Writing – original draft, Methodology, Formal analysis, Data curation. **A. Ström:** Writing – review & editing, Supervision, Methodology. **A. Jiménez-Quero:** Writing – review & editing, Writing – original draft, Validation, Supervision, Resources, Funding acquisition, Conceptualization.

Declaration of competing interest

The authors declare that they have no known competing financial interests or personal relationships that could have appeared to influence the work reported in this paper.

Acknowledgements

The authors gratefully acknowledge Alginor ASA for kindly providing the raw algal biomass used in this study. We sincerely thank Dr. Miroslava Atanasova (Møreforsking AS, Norway) for her supervision and project management of the bioactive assays, as well as Manuel Bartolomé Díaz (Universidad de Castilla-La Mancha, Spain) for his expert support in the downstream processing experiments. The authors acknowledge funding from the CIRCALGAE project (Grant Agreement No. 101060607) under the Horizon Europe programme (CL6-2021-CIRCBIO-01).

Appendix A. Supplementary data

Supplementary data to this article can be found online at https://doi.org/10.1016/j.biteb.2026.102928.

Data availability

The data supporting the findings of this study are available in the CIRCALGAE Zenodo repository, hosted by Zenodo, and can be accessed via the corresponding project community.

References

Ahmad, T., Eapen, M.S., Ishaq, M., Park, A.Y., Karpiniec, S.S., Stringer, D.N., Sohal, S.S., Fitton, J.H., Guven, N., Caruso, V., Eri, R., 2021. Anti-inflammatory activity of fucoidan extracts in vitro. Mar. Drugs 19, 702. https://doi.org/10.3390/md19120702.

Aït-Kaddour, A., Hassoun, A., Tarchi, I., Loudiyi, M., Boukria, O., Cahyana, Y., Ozogul, F., Khwaldia, K., 2024. Transforming plant-based waste and by-products into valuable products using various "Food Industry 4.0" enabling technologies: a literature review. Sci. Total Environ. 955, 176872. https://doi.org/10.1016/J.SCITOTENV.2024.176872.

Alboofetileh, M., Rezaei, M., Tabarsa, M., You, S.G., Mariatti, F., Cravotto, G., 2019. Subcritical water extraction as an efficient technique to isolate biologically-active fucoidans from *Nizamuddinia zanardinii*. Int. J. Biol. Macromol. 128, 244–253. https://doi.org/10.1016/j.ijbiomac.2019.01.119.

Ali, M.S., Haq, M., Park, S.W., Han, J.M., Kim, J.W., Choi, M.S., Lee, S.M., Park, J.S., Chun, M.S., Lee, H.J., Chun, B.S., 2025. Recent advances in recovering bioactive compounds from macroalgae and microalgae using subcritical water extraction: prospective compounds and biological activities. Food Chem. 469, 142602. https://doi.org/10.1016/J.FOODCHEM.2024.142602.

Álvarez-Viñas, M., Rodríguez-Seoane, P., Flórez-Fernández, N., Ma, Torres, D., Díaz-Reinoso, B., Moure, A., Domínguez, H., 2020. Subcritical Water for the Extraction and Hydrolysis of Protein and Other Fractions in Biorefineries from Agro-food Wastes and Algae: A Review. https://doi.org/10.1007/s11947-020-02536-4/Published.

Angell, A.R., Mata, L., de Nys, R., Paul, N.A., 2016. The protein content of seaweeds: a universal nitrogen-to-protein conversion factor of five. J. Appl. Phycol. 28, 511–524. https://doi.org/10.1007/s10811-015-0650-1.

Apostolova, E., Lukova, P., Baldzhieva, A., Katsarov, P., Nikolova, M., Iliev, I., Peychev, L., Trica, B., Oancea, F., Delattre, C., Kokova, V., 2020. Immunomodulatory and anti-inflammatory effects of fucoidan: a review. Polymers 12, 2338. https://doi.org/10.3390/polym12102338.

Baghel, R.S., Reddy, C.R.K., Singh, R.P., 2021. Seaweed-based cellulose: applications, and future perspectives. Carbohydr. Polym. 267, 118241. https://doi.org/10.1016/J.CARBPOL.2021.118241.

Biermann, C.J., 1988. Hydrolysis and other Cleavages of Glycosidic Linkages in Polysaccharides. Adv. Carbohydr. Chem. Biochem. 46, 251–271. https://doi.org/10.1016/S0065-2318(08)60168-7.

Blunden, G., 1993. Marine algae as sources of biologically active compounds. Interdiscip. Sci. Rev. 18, 73–80. https://doi.org/10.1179/isr.1993.18.1.73.

Bojorges, H., Fabra, M.J., López-Rubio, A., Martínez-Abad, A., 2022. Alginate industrial waste streams as a promising source of value-added compounds valorization. Sci. Total Environ. 838, 156394. https://doi.org/10.1016/J.SCITOTENV.2022.156394.

Bradford, M.M., 1976. A rapid and sensitive method for the quantitation of microgram quantities of protein utilizing the principle of protein-dye binding. Anal. Biochem. 72, 248–254. https://doi.org/10.1016/0003-2697(76)90527-3.

Brescia, P.J., 2021. Determination of Antioxidant Potential Using an Oxygen Radical Absorbance Capacity (ORAC) Assay with Synergy™ H4. Winooski, VT (USAI).

Carvalho, L.G., McDougall, G., Allwood, W., Sungurtas, J., Verrall, S., Stewart, D., Neilson, K., O'Byrne, M., 2023. Tissues and industrial co-products formed during alginate extraction from *Laminaria hyperborea* provide different metabolite profiles depending on harvest season. J. Appl. Phycol. 35, 849–865. https://doi.org/10.1007/s10811-022-02895-9.

Cebrián-Lloret, V., Metz, M., Martínez-Abad, A., Knutsen, S.H., Ballance, S., López-Rubio, A., Martínez-Sanz, M., 2022. Valorization of alginate-extracted seaweed biomass for the development of cellulose-based packaging films. Algal Res. 61, 102576. https://doi.org/10.1016/J.ALGAL.2021.102576.

Cheng, Y., Xue, F., Yu, S., Du, S., Yang, Y., Lovillo, M.P., Carrera Fernández, C.A., Ruiz Rodríguez, A., 2021. Subcritical water extraction of natural products. Molecules 26, 4004. https://doi.org/10.3390/MOLECULES26134004, 2021, Vol. 26, Page 4004.

Costa, J.M., Strieder, M.M., Saldaña, M.D.A., Rostagno, M.A., Forster-Carneiro, T., 2023. Recent advances in the processing of agri-food by-products by subcritical water. Food Bioprocess Technol. 16, 2705–2724. https://doi.org/10.1007/S11947-023-03071-8, 2023 16: 12.

Draget, K.I., Skjåk-Bræk, G., Smidsrød, O., 1997. Alginate based new materials. Int. J. Biol. Macromol. 21, 47–55. https://doi.org/10.1016/S0141-8130(97)00040-8.

Eger, A.M., Marzinelli, E.M., Beas-Luna, R., Blain, C.O., Blamey, L.K., Byrnes, J.E.K., Carnell, P.E., Choi, C.G., Hessing-Lewis, M., Kim, K.Y., Kumagai, N.H., Lorda, J., Moore, P., Nakamura, Y., Pérez-Matus, A., Pontier, O., Smale, D., Steinberg, P.D., Vergés, A., 2023. The value of ecosystem services in global marine kelp forests. Nat. Commun. 14, 1894. https://doi.org/10.1038/s41467-023-37385-0.

Espro, C., Paone, E., Mauriello, F., Gotti, R., Uliassi, E., Bolognesi, M.L., Rodríguez-Padrón, D., Luque, R., 2021. Sustainable production of pharmaceutical, nutraceutical and bioactive compounds from biomass and waste. Chem. Soc. Rev. 50, 11191–11207. https://doi.org/10.1039/D1CS00524C.

Garcia-Vaquero, M., Rajauria, G., Miranda, M., Sweeney, T., Lopez-Alonso, M., O'doherty, J., 2021. Seasonal variation of the proximate composition, mineral content, fatty acid profiles and other phytochemical constituents of selected brown macroalgae. Mar. Drugs 19, 204. https://doi.org/10.3390/MD19040204/S1.

Getachew, A.T., Holdt, S.L., Meyer, A.S., Jacobsen, C., 2022. Effect of extraction temperature on pressurized liquid extraction of bioactive compounds from *Fucus vesiculosus*. Mar. Drugs 20. https://doi.org/10.3390/md20040263.

Gottinger, A., Ladu, L., Quitzow, R., 2020. Studying the transition towards a Circular Bioeconomy—a systematic literature review on transition studies and existing barriers. Sustainability 12, 8990. https://doi.org/10.3390/SU12218990, 2020, Vol. 12, Page 8990.

Greenhill, L., Sundnes, F., Karlsson, M., 2021. Towards sustainable management of kelp forests: an analysis of adaptive governance in developing regimes for wild kelp harvesting in Scotland and Norway. Ocean Coast. Manag. 212, 105816. https://doi.org/10.1016/j.ocecoaman.2021.105816.

Hahn, T., Lang, S., Ulber, R., Muffler, K., 2012. Novel procedures for the extraction of fucoidan from brown algae. Process Biochem. 47, 1691–1698. https://doi.org/10.1016/j.procbio.2012.06.016.

Harmsen, P., 2014. Kelp2Plastics Converting Sugar Kelp Into Biobased Plastics.

Hunter, C.A., Jones, S.A., 2015. IL-6 as a keystone cytokine in health and disease. Nat. Immunol. 16, 448–457. https://doi.org/10.1038/ni.3153.

Johnson, J.B., Mani, J.S., Naiker, M., 2022. Development and validation of a 96-well microplate assay for the measurement of total phenolic content in ginger extracts. Food Anal. Methods 15, 413–420. https://doi.org/10.1007/s12161-021-02127-9.

Ko, M.J., Nam, H.H., Chung, M.S., 2020. Subcritical water extraction of bioactive compounds from *Orostachys japonicus* a. Berger (Crassulaceae). Sci. Rep. 10, 1–10. https://doi.org/10.1038/S41598-020-67508-2. SUBJMETA=2668,449,631; KWRD=PLANT+ECOLOGY,PLANT+SCIENCES.

Kopplin, G., Rokstad, A.M., Mélida, H., Bulone, V., Skjåk-Bræk, G., Aachmann, F.L., 2018. Structural characterization of fucoidan from *Laminaria hyperborea*: assessment of coagulation and inflammatory properties and their structure-function relationship. ACS Appl. Bio Mater. 1, 1880–1892. https://doi.org/10.1021/acsabm.8b00436.

Leyva-Jiménez, F.J., Fernandez-Ochoa, A., Cádiz-Gurrea, M.D.L.L., Lozano-Sánchez, J., Oliver-Simancas, R., Alañón, M.E., Arráez-Román, D., 2022. Application of response surface methodologies to optimize high-added value products developments: Cosmetic formulations as an example. Antioxidants 11 (8), 1552.

Li, Y., Zheng, Y., Zhang, Y., Yang, Y., Wang, P., Imre, B., Wong, A.C.Y., Hsieh, Y.S.Y., Wang, D., 2021. Brown algae carbohydrates: Structures, pharmaceutical properties, and research challenges. Mar. Drugs 19. https://doi.org/10.3390/MD19110620.

Liu, Z., de Souza, T.S.P., Holland, B., Dunshea, F., Barrow, C., Suleria, H.A.R., 2023. Valorization of food waste to produce value-added products based on its bioactive compounds. Processes 11, 840. https://doi.org/10.3390/PR11030840, 2023, Vol. 11, Page 840.

Liyanapathirana, C., Shahidi, F., 2005. Optimization of extraction of phenolic compounds from wheat using response surface methodology. Food Chem. 93, 47–56. https://doi.org/10.1016/j.foodchem.2004.08.050.

Majeed, T., Shabir, I., Srivastava, S., Maqbool, N., Dar, A.H., Jan, K., Pandey, V.K., Shams, R., Bashir, I., Dash, K.K., Hanan, E., Wani, N.R., 2024. Valorization of food wastes by implementation of subcritical water extraction: a comprehensive review. Trends Food Sci. Technol. 143, 104316. https://doi.org/10.1016/J.TIFS.2023.104316.

Martínez-Abad, A., Jiménez-Quero, A., Wohlert, J., Vilaplana, F., 2020. Influence of the molecular motifs of mannan and xylan populations on their recalcitrance and organization in spruce softwoods. Green Chem. 22, 3956–3970. https://doi.org/10.1039/D0GC01207F.

Mohd Fauziee, N.A., Chang, L.S., Wan Mustapha, W.A., Md Nor, A.R., Lim, S.J., 2021. Functional polysaccharides of fucoidan, laminaran and alginate from Malaysian brown seaweeds (*Sargassum polycystum*, *Turbinaria ornata* and *Padina boryana*). Int. J. Biol. Macromol. 167, 1135–1145. https://doi.org/10.1016/J.IJBIOMAC.2020.11.067.

Mohd Thani, N., Mustapa Kamal, S.M., Sulaiman, A., Taip, F.S., Omar, R., Izhar, S., 2020. Sugar recovery from food waste via sub-critical water treatment. Food Rev. Int. 36, 241–257. https://doi.org/10.1080/87559129.2019.1636815;WGROUP:STRING:PUBLICATION.

Moloeznik Paniagua, D., Krenz, L.M.M., Libra, J.A., Korf, N., Rotter, V.S., 2024. Towards a high-quality fertilizer based on algae residues treated via hydrothermal carbonization. Trends on how process parameters influence inorganics. Biochar 6, 1–25. https://doi.org/10.1007/S42773-024-00357-8/TABLES/6.

Myers, H. Raymond, M., C.D., A.-C., C.C., 2016a. Process and Product Optimization Using Designed Experiments, 4th ed. In: Wiley Series in Probability and Statistics. John Wiley & Sons Inc., New Jersey. 4th ed.. John Wiley & Sons, 2016.

Myers, R.H., Montgomery, D.C., Anderson-Cook, C.M., 2016b. Response Surface Methodology: Process and Product Optimization, Fourth. ed. In: Wiley Series in Probability and Statistics. John Wiley & Sons Inc., New Jersey. 4th ed.,. John Wiley & Sons, 2016.

Onyianta, A.J., O'Rourke, D., Sun, D., Popescu, C.M., Dorris, M., 2020. High aspect ratio cellulose nanofibrils from macroalgae Laminaria hyperborea cellulose extract via a zero-waste low energy process. Cellulose 27, 7997–8010. https://doi.org/10.1007/S10570-020-03223-5/FIGURES/9.

Pan, Z., Zeng, B., Yu, G., Teng, J., Zhang, H., Shen, L., Yang, L., Lin, H., 2022. Mechanistic insights into Ca-alginate gel-associated membrane fouling affected by ethylene diamine tetraacetic acid (EDTA). Sci. Total Environ. 842, 156912. https://doi.org/10.1016/J.SCITOTENV.2022.156912.

Plaza, M., Amigo-Benavent, M., del Castillo, M.D., Ibáñez, E., Herrero, M., 2010a. Neoformation of antioxidants in glycation model systems treated under subcritical water extraction conditions. Food Res. Int. 43, 1123–1129. https://doi.org/10.1016/J.FOODRES.2010.02.005.

Plaza, M., Amigo-Benavent, M., del Castillo, M.D., Ibáñez, E., Herrero, M., 2010b. Facts about the formation of new antioxidants in natural samples after subcritical water extraction. Food Res. Int. 43, 2341–2348. https://doi.org/10.1016/J.FOODRES.2010.07.036.

Re, R., Pellegrini, N., Proteggente, A., Pannala, A., Yang, M., Rice-Evans, C., 1999. Antioxidant activity applying an improved ABTS radical cation decolorization assay. Free Radic. Biol. Med. 26, 1231–1237. https://doi.org/10.1016/S0891-5849(98)00315-3.

Remya, R.R., Samrot, A.V., Kumar, S.S., Mohanavel, V., Karthick, A., Chinnaiyan, V.K., Umapathy, D., Muhibbullah, M., 2022. Bioactive potential of brown algae. Adsorpt. Sci. Technol. 2022. https://doi.org/10.1155/2022/9104835.

Sandoval-Gallardo, J.M., Osuna-Ruiz, I., Martínez-Montaño, E., Hernández, C., Hurtado-Oliva, M.Á., Valdez-Ortiz, Á., Rios-Herrera, G.D., Salazar-Leyva, J.A., Ramírez-Pérez, J.S., 2020. Influence of enzymatic hydrolysis conditions on biochemical and antioxidant properties of pacific thread herring (*Ophistonema libertate*) hydrolysates. CyTA - Journal of Food 18, 392–400. https://doi.org/10.1080/19476337.2020.1767694.

Saravana, P.S., Tilahun, A., Gerenew, C., Tri, V.D., Kim, N.H., Kim, G. Do, Woo, H.C., Chun, B.S., 2018. Subcritical water extraction of fucoidan from *Saccharina japonica*: optimization, characterization and biological studies. J. Appl. Phycol. 30, 579–590. https://doi.org/10.1007/s10811-017-1245-9.

Savić Gajić, I.M., Savić, I.M., Ivanovska, A.M., Vunduk, J.D., Mihalj, I.S., Svirčev, Z.B., 2024. Improvement of alginate extraction from brown seaweed (*Laminaria digitata*

L.) and valorization of its remaining ethanolic fraction. Mar. Drugs 22, 280. https://doi.org/10.3390/md22060280.

Schiener, P., Black, K.D., Stanley, M.S., Green, D.H., 2015. The seasonal variation in the chemical composition of the kelp species *Laminaria digitata*, *Laminaria hyperborea*, *Saccharina latissima* and *Alaria esculenta*. J. Appl. Phycol. 27, 363–373. https://doi.org/10.1007/S10811-014-0327-1/TABLES/2.

Schipfer, F., Burli, P., Fritsche, U., Hennig, C., Stricker, F., Wirth, M., Proskurina, S., Serna-Loaiza, S., 2024. The circular bioeconomy: a driver for system integration. Energy Sustain. Soc. 14, 1–19. https://doi.org/10.1186/S13705-024-00461-4/METRICS.

Shao, Q., Deng, Y., shen, H., Fang, H., Zhao, X., 2011. Optimization of polysaccharides extraction from *Tetrastigma hemsleyanum* Diels et Gilg using response surface methodology. Int. J. Biol. Macromol. 49, 958–962. https://doi.org/10.1016/J.IJBIOMAC.2011.08.015.

Singleton, V.L., Orthofer, R., Lamuela-Raventós, R.M., 1999. [14] Analysis of total phenols and other oxidation substrates and antioxidants by means of folin-ciocalteu reagent, pp. 152–178. https://doi.org/10.1016/S0076-6879(99)99017-1.

Smale, D.A., Pessarrodona, A., King, N., Burrows, M.T., Yunnie, A., Vance, T., Moore, P., 2020. Environmental factors influencing primary productivity of the forest-forming kelp *Laminaria hyperborea* in the northeast Atlantic. Sci. Rep. 10, 12161. https://doi.org/10.1038/s41598-020-69238-x.

Smidsrod, O., Skjakbrk, G., 1990. Alginate as immobilization matrix for cells. Trends Biotechnol. 8, 71–78. https://doi.org/10.1016/0167-7799(90)90139-O.

Stacey, N., Gibson, E., Loneragan, N.R., Warren, C., Wiryawan, B., Adhuri, D.S., Steenbergen, D.J., Fitriana, R., 2021. Developing sustainable small-scale fisheries livelihoods in Indonesia: Trends, enabling and constraining factors, and future opportunities. Mar. Policy 132, 104654. https://doi.org/10.1016/j.marpol.2021.104654.

Trigueros, E., Ramos, C., Alonso-Riaño, P., Beltrán, S., Sanz, M.T., 2023. Subcritical water treatment for valorization of the red algae residue after agar extraction: scale-up from laboratory to pilot plant. Ind. Eng. Chem. Res. 62, 3503–3514. https://doi.org/10.1021/ACS.IECR.2C04132/ASSET/IMAGES/LARGE/IE2C04132_0010.JPEG.

Trigueros, E., Oliveira, A.P., Andrade, P.B., Videira, R.A., de Pinho, P.G., Sanz, M.T., Beltrán, S., 2024. Exploring the bioactive potential of algae residue extract via subcritical water extraction: Insights into chemical composition and biological activity. Food Chem. 458, 140310. https://doi.org/10.1016/J.FOODCHEM.2024.140310.

Wekre, M.E., Holmelid, B., Underhaug, J., Pedersen, B., Kopplin, G., Jordheim, M., 2023. Characterization of high value products in the side-stream of *Laminaria hyperborea* alginate production - Targeting the phenolic content. Algal Res. 72, 103109. https://doi.org/10.1016/j.algal.2023.103109.

Weremfo, A., Abassah-Oppong, S., Adulley, F., Dabie, K., Seidu-Larry, S., 2023. Response surface methodology as a tool to optimize the extraction of bioactive compounds from plant sources. J. Sci. Food Agric. 103 (1), 26–36.

Wood, I.P., Elliston, A., Ryden, P., Bancroft, I., Roberts, I.N., Waldron, K.W., 2012. Rapid quantification of reducing sugars in biomass hydrolysates: Improving the speed and precision of the dinitrosalicylic acid assay. Biomass Bioenergy 44, 117–121.

Yang, L., Qu, H., Mao, G., Zhao, T., Li, F., Zhu, B., Zhang, B., Wu, X., 2013. Optimization of subcritical water extraction of polysaccharides from *Grifola frondosa* using response surface methodology. Pharmacogn. Mag. 9, 120. https://doi.org/10.4103/0973-1296.111262.

Yilmaz-Turan, S., Gál, T., Lopez-Sanchez, P., Martinez, M.M., Menzel, C., Vilaplana, F., 2023. Modulating temperature and pH during subcritical water extraction tunes the molecular properties of apple pomace pectin as food gels and emulsifiers. Food Hydrocoll. 145, 109148. https://doi.org/10.1016/J.FOODHYD.2023.109148.

Yu, X. mei, Zhu, P., Zhong, Q. ping, Li, M. ying, Ma, H. ruo, 2014. Subcritical water extraction of antioxidant phenolic compounds from XiLan olive fruit dreg. J. Food Sci. Technol. 52, 5012. https://doi.org/10.1007/S13197-014-1551-Z.

Zhu, G., Zhu, X., Fan, Q., Wan, X., 2011. Recovery of biomass wastes by hydrolysis in sub-critical water. Resour. Conserv. Recycl. 55, 409–416. https://doi.org/10.1016/J.RESCONREC.2010.12.012.